NAVAL POSTGRADUATE SCHOOL

MONTEREY, CALIFORNIA

THESIS

A VERIFICATION OF AEROSOL OPTICAL DEPTH RETRIEVAL USING THE TERRA SATELLITE

By

Brett D. Cimbora

June 2012

Thesis Advisor:	Phillip A. Durkee
Second Reader:	Kurt E. Nielsen

THIS PAGE INTENTIONALLY LEFT BLANK

REPORT DOCUMENTATION PAGE			Form Approved OMB No. 0704-0188
Public reporting burden for this collection of information is estimated to average 1 hour per response, including the time for reviewing instruction, searching existing data sources, gathering and maintaining the data needed, and completing and reviewing the collection of information. Send comments regarding this burden estimate or any other aspect of this collection of information, including suggestions for reducing this burden, to Washington headquarters Services, Directorate for Information Operations and Reports, 1215 Jefferson Davis Highway, Suite 1204, Arlington, VA 22202-4302, and to the Office of Management and Budget, Paperwork Reduction Project (0704-0188) Washington DC 20503.			
1. AGENCY USE ONLY ***(Leave blank)***	**2. REPORT DATE** June 2012	**3. REPORT TYPE AND DATES COVERED** Master's Thesis	
4. TITLE AND SUBTITLE A Verification Of Aerosol Optical Depth Retrieval Using The Terra Satellite		**5. FUNDING NUMBERS**	
6. AUTHOR(S) Brett Cimbora			
7. PERFORMING ORGANIZATION NAME(S) AND ADDRESS(ES) Naval Postgraduate School Monterey, CA 93943-5000		**8. PERFORMING ORGANIZATION REPORT NUMBER**	
9. SPONSORING /MONITORING AGENCY NAME(S) AND ADDRESS(ES) N/A		**10. SPONSORING/MONITORING AGENCY REPORT NUMBER**	
11. SUPPLEMENTARY NOTES The views expressed in this thesis are those of the author and do not reflect the official policy or position of the Department of Defense or the U.S. Government. IRB Protocol number _____N/A_____.			
12a. DISTRIBUTION / AVAILABILITY STATEMENT Approved for public release; distribution is unlimited.		**12b. DISTRIBUTION CODE** A	

13. ABSTRACT (maximum 200 words)

A method for sensing retrieval of Aerosol Optical Depth (AOD) was investigated by Vincent (2006). This technique is known as the Shadow Method. Using high-resolution commercial satellite imagery, Vincent was able to calculate AOD values by measuring the radiance of a scene in and out of a shadow. Over the last five years, several advancements have been made to validate the Shadow Method. Using the MODerate resolution Imaging Spectrometer (MODIS), scenes were analyzed over desert regions to exploit shadows generated by clouds and terrain. The results were quickly compiled using MATLAB. Results confirm that the Shadow Method is capable of producing AOD values.

14. SUBJECT TERMS Aerosol optic depth; satellite sensing			**15. NUMBER OF PAGES** 55
			16. PRICE CODE
17. SECURITY CLASSIFICATION OF REPORT Unclassified	**18. SECURITY CLASSIFICATION OF THIS PAGE** Unclassified	**19. SECURITY CLASSIFICATION OF ABSTRACT** Unclassified	**20. LIMITATION OF ABSTRACT** UU

NSN 7540-01-280-5500 Standard Form 298 (Rev. 2-89)
Prescribed by ANSI Std. 239-18

THIS PAGE INTENTIONALLY LEFT BLANK

Approved for public release; distribution is unlimited.

A VERIFICATION OF AEROSOL OPTICAL DEPTH RETRIEVAL USING THE TERRA SATELLITE

Brett D. Cimbora
Captain, United States Air Force
B.S., Florida State University, 2003

Submitted in partial fulfillment of the
requirements for the degree of

MASTER OF SCIENCE IN METEOROLOGY

from the

NAVAL POSTGRADUATE SCHOOL
June 2012

Author: Brett D. Cimbora

Approved by: Phillip A. Durkee
Thesis Advisor

Kurt E. Nielsen
Second Reader

Wendell A. Nuss
Chair, Department of Meteorology

THIS PAGE INTENTIONALLY LEFT BLANK

ABSTRACT

A method for sensing retrieval of Aerosol Optical Depth (AOD) was investigated by Vincent (2006). This technique is known as the Shadow Method. Using high-resolution commercial satellite imagery, Vincent was able to calculate AOD values by measuring the radiance of a scene in and out of a shadow. Over the last five years, several advancements have been made to validate the Shadow Method. Using the MODerate resolution Imaging Spectrometer (MODIS), scenes were analyzed over desert regions to exploit shadows generated by clouds and terrain. The results were quickly compiled using MATLAB. Results confirm that the Shadow Method is capable of producing AOD values.

THIS PAGE INTENTIONALLY LEFT BLANK

TABLE OF CONTENTS

THIS PAGE INTENTIONALLY LEFT BLANK

LIST OF FIGURES

LIST OF ACRONYMS AND ABBREVIATIONS

AERONET	Aerosol Robotic Network
AOD	Aerosol Optical Depth
ENVI	Environment for Visualizing Images
LP DAAC	Land Process Distributed Active Archive Center
MAR	Mean Aerosol Reflectance
MATLAB	Mathwork's Matrix Laboratory
MODIS	MODerate resolution Imaging Spectrometer
MROD	Molecular Rayleigh Optical Depth
NASA	National Aeronautics and Space Administration
POI	Principles of Invariance
ROD	Rayleigh Optical Depth
ROI	Region of Interest
TACSAT	Tactical Satellite
TOA	Top-of-Atmosphere
TOD	Total Optical Depth
USGS	United States Geological Survey
UTC	Coordinated Universal Time

THIS PAGE INTENTIONALLY LEFT BLANK

LIST OF SYMBOLS

δ_0	Total Optical Depth
μ	Cosine of sensor zenith angle
μ_0	Cosine of solar zenith angle
r_s	Surface reflectance
$\bar{r}$	Mean aerosol reflectance
F_0	Spectral solar irradiance
L_d	Radiance difference
$\tilde{\omega}$	Single scatter albedo
P	Scattering phase function
Θ	Scattering angle
g	Asymmetry parameter
(μ', ϕ')	Cosine of incident zenith and azimuth angles
(μ'', ϕ'')	Cosine of resultant zenith and azimuth angles
δ_R	Rayleigh optical depth
H	Height above sea level
λ	Wavelength
p	Atmospheric pressure
p_0	Sea-level reference pressure (1013.25 hPa)
L_λ	Spectral radiance
θ	Angle

THIS PAGE INTENTIONALLY LEFT BLANK

ACKNOWLEDGMENTS

I would like to thank Professors Philip Durkee and Wendell Nuss for their support and understanding during this entire process. There were several limitations early on in the research and they were very patient and quick to come up with a solution. Kurt Nielsen spent time with me in the lab, helping with the data analysis. Mary Jordan, the local MATLAB expert, helped make the code user-friendly. During my time at NPS, many challenges presented themselves and I was amazed at the support that I received from the Meteorology Department faculty. My wife, Wendy offered the greatest support, cheering me along the way and keeping me focused. I could not have made it without her or the Grace of God.

THIS PAGE INTENTIONALLY LEFT BLANK

I. INTRODUCTION

The earth's atmosphere is comprised of matter in three physical states: liquid, gas and solid. Atmospheric matter ranging from a few nanometers to 100 micrometers in diameter, is classified as an aerosol (Waghelstein 2010). Concentrations of aerosols can vary greatly with respect to time and the environment, but can reach numerical densities as high as $10^7 - 10^8$ cm^{-3} (Seinfeld 2006). These relatively small particles can originate from either natural or man-made sources. Naturally occurring aerosols most often appear in the form of volcanic ash, dust, smoke, pollen and sea spray. Man-made aerosols are most commonly found to include combustion-generated byproducts such as exhaust from automobile and power generation facilities.

With such great variation in concentration and size, it is important to understand the impact aerosols have on the environment. Aerosols alter the radiation budget of the earth's atmosphere by scattering or absorbing direct solar radiation. How much they can absorb and scatter varies between aerosol types and is most dependent on shape and size (Seinfeld 2006). Greater aerosol concentrations can also increase the amount of cloud condensation nuclei in a region. This produces more cloud cover, higher cloud reflectance, lower visibility and colder atmospheric and surface temperatures

Unfortunately, aerosol measurement is not an easy task. Dedicated and expensive equipment is required to measure aerosol optical depth (AOD), but is impractical for use outside of academia and research. With large variations in aerosol content from place to place and time to time, these sensors are limited in delivering relevant information and usually have small temporal and spatial windows. Also, most countries do not have the funds or the interest to invest in dedicated sensors, so obtaining measurements in military-sensitive areas is a difficult challenge.

One method that is gaining momentum is Vincent's Shadow Method (2006). Using high-resolution commercial satellite imagery, Vincent was able to calculate AOD values by measuring the radiance of a scene in and out of a shadow. Research in the last five years has further validated and refined this process. Evans (2007) analyzed the

output of the technique for various ground surfaces using QuickBird multi-spectral and panchromatic sensor channels. Dombrock (2007) developed a method to automate many of the calculations the Shadow Method relied on to obtain AOD values more quickly. Sweat (2008) showed that shadows from cloud cover could be used to calculate radiance values needed for AOD retrieval. Rivenbark (2009) studied the low-bias trend the Shadow Method was producing when compared to in-situ observations and determined better selection criteria for shadow generators to help reduce the disparity. Belson (2010) wrote a sophisticated code that automated the entire process, from user-defined shadow selection to AOD retrieval. Waghelstein (2010) departed from the high spatial resolution sensors and analyzed scenes taken with the TACSAT-3 satellite, launched on May 19, 2009, with the onboard Advanced Responsive Tactically Effective Military Imaging Spectrometer (ARTEMIS). This hyper-spectral imagery provided a unique opportunity in that images were low in spatial resolution, but were high in spectral resolution.

This research originally started using hyper-spectral imagery, but the Department of Defense mandated that classified data could not be transferred to removable media. It was then where the decision was made to use Moderate Resolution Imaging Spectrometer (MODIS) imagery. According to NASA, MODIS is a key instrument aboard the Terra and Aqua satellites. Terra's orbit around the Earth is timed so that it passes from north to south across the equator in the morning, while Aqua passes south to north over the equator in the afternoon. Terra MODIS and Aqua MODIS are viewing the entire Earth's surface every 1 to 2 days, acquiring data in 36 spectral bands, or groups of wavelengths.

II. BACKGROUND

A. PREVIOUS RESEARCH

1. Contrast Reduction Method

One of the first attempts to identify aerosol optical depth by remote sensing was done by Odell and Weinman (1975) via the Contrast Reduction Method. This method produced theoretical AOD values by using a contrast modulation function, radiance values from two distinct objects with different albedo, mean surface reflectance, sun-sensor geometry and a specific aerosol model. Kaufman and Joseph (1982) continued this technique using a "Two Halves" approach that relied on imagery with obvious discontinuity in albedo, like a coastline or forest boundary. Both of these methods were heavily dependent.

2. Dark Object Method

The Dark Object Method uses surface features with low reflectance to find optical depth contributions from aerosols. Any measured radiance beyond the assumed surface albedo of a low surface reflectance feature, like a deep body of water or dense forest region, is attributed to aerosol reflection along the path. Kaufman and Sendra (1988) created an algorithm to apply the technique over dense vegetation. Much like the Contrast Reduction Method, the Dark Object Method has the tendency to produce large errors due to false assumptions in aerosol models and surface albedo. This method also cannot be used in areas of high surface reflectance like deserts or urban areas.

The Dark Object Method was expounded upon when Hsu et al. (2004) developed the "Deep Blue" Method, which sought to find AOD values in areas of high surface reflectance. Hsu's team exploited the fact that bright objects with high reflectance often reflected back strongly in longer wavelengths, but were not as reflective in the shorter wavelengths that corresponded to the satellite's blue channel. By using sensors with two or more blue channels, AOD values could be derived, depending on if the surface

reflectance was not too high. In the best cases, the Deep Blue Method achieved values within 20% of NASA's Aeronet values, but was limited to platforms with multiple blue channels.

3. Multi-angle Method

Another approach aimed at finding AOD was the Multi-angle Method, developed by Veefkind in 1998. Veefkind conceived a way to retrieve AOD in areas of high surface reflectance without the need for multi-blue satellite channels. This method used satellite platforms capable of multiple viewing angles collected simultaneously. By collecting images at different angles simultaneously, atmospheric columns from each image could be categorized and used to derive AOD. While the process proved to be accurate, both in high and low surface reflectance environments, it had two major limitations. First, the method was restricted to multi-angle sensors. Secondly, these sensors were restricted to three- to nine-day revisit times due to their orbital parameters (Veefkind et al., 1998), making tactical use over a sustained region of interest unfeasible.

B. SHADOW METHOD

1. Introduction

Unless otherwise cited, the information provided in this description of the Shadow Method was taken from Vincent (2006). The Shadow Method exploits the shadows cast by buildings, clouds and terrain in high-resolution imagery to measure total optical depth. This research sought to exploit shadows cast by clouds and mountains over desert terrain. Several commercially-available satellites have sufficient shadow detection capability. This research used Moderate Resolution Imaging Spectrometer (MODIS) imagery aboard the Terra Satellite.

In order to use the Shadow Method, it is important to understand the components used to get the total and aerosol optical depths. Figure 1 depicts the basic components of radiance received at a satellite, both in-shadow and out-of-shadow. *Direct transmission* is the amount of radiation that travels from the sun to the ground, then reflected back to

the sensor. *Diffuse transmission* is the amount of radiation that has reached the sensor after it has been scattered by some atmospheric component and reflected back to the sensor. *Diffuse reflection* is similar to diffuse transmission, except the radiation goes through another scatter by some atmospheric component before it is reflected back to the sensor. All three components make up the out-of-shadow signal, while the in-shadow signal lacks the direct transmission component. Taking the difference between the shaded and unshaded photon budgets, we get the difference in observed radiance as a function of surface reflectance, mean aerosol reflectance, solar zenith angle, satellite zenith angle, solar irradiance and total optical depth (TOD). The TOD portion of the signal is the key to calculating optical depth.

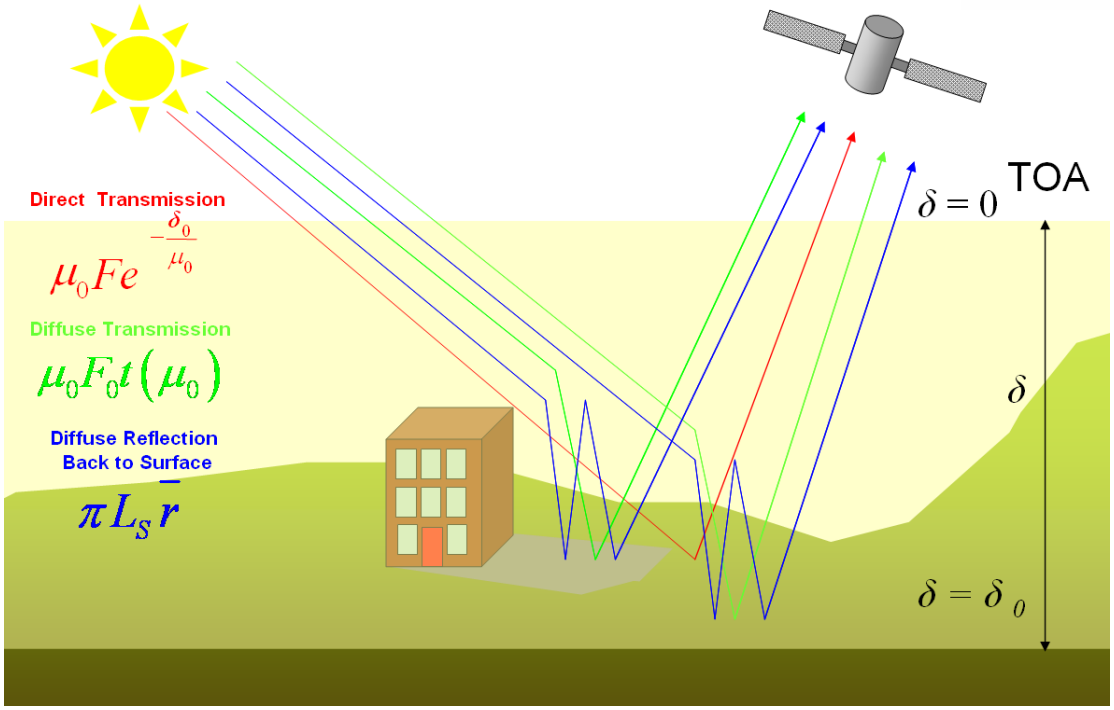

Figure 1. Depiction of the difference between the in-shadow and out-of-shadow signal received by a satellite. Subtracting the two signals isolates the direct transmission component of the signal which can be used to calculate total optical depth (from Vincent 2006).

2. General Calculation

In order to derive the AOD using the Shadow Method, a governing equation must be used to account for the flux densities that contribute to the top of the atmosphere (TOA) radiance. Vincent (2206) provides extensive proof in his work, which will be summarized as follows:

The three flux densities in Figure 1 are:

Direct Transmission is given as,

$$\mu_0 F_0 e^{-\delta 0/\mu_0} \quad \textbf{(1)}$$

where μ_0 is the cosine of the solar zenith angle, F_0 is the spectral solar radiant flux density and $\delta 0$ is the optical depth of the atmosphere.

Diffuse Transmission is given as,

$$\mu_0 F_0 t(\delta_0, \mu_0) \quad \textbf{(2)}$$

where *t* is the transmittance.

Diffuse Reflection is given as,

$$\pi L_s \bar{r} \quad \textbf{(3)}$$

where L_s is the surface radiance and $\bar{r}$ is the mean aerosol reflectance.

Given these three quantities, the total flux density can be expressed as,

$$\pi L_s = r_s(\mu_0 F_0 e^{-\delta 0/\mu_0} + \mu_0 F_0 t(\delta_0, \mu_0) + \pi L_s \bar{r}) \quad \textbf{(4)}$$

where r_s is the surface reflectance.

Solving for the Surface Radiance, L_s, yields,

$$L_s = \frac{r_s}{1 - r_s \bar{r}} \frac{\mu_0 F_0}{\pi} (e^{-\delta 0/\mu_0} + t(\delta_0, \mu_0)). \quad \textbf{(5)}$$

For the satellite to sense the measured surface radiance of an unshaded region of the scene, the term must be multiplied by another attenuation coefficient (atmospheric optical depth) as it travels through the atmosphere a second time to reach the sensor. Thus, the unshaded surface radiance can be expressed as,

$$L_s^{unshaded} = \left[\frac{r_s}{1 - r_s \bar{r}} \frac{\mu_0 F_0}{\pi} (e^{-\delta 0/\mu 0} + t(\delta_0, \mu_0)) \right] e^{-\delta 0/\mu 0} \quad \textbf{(6)}$$

The additional extinction term is dependent on the viewing angle, where μ is the cosine of the sensor zenith angle.

To obtain the measured radiance of a shadow region, the equation,

$$L_s^{shaded} = \left[\frac{r_s}{1 - r_s \bar{r}} \frac{\mu_0 F_0}{\pi} (t(\delta_0, \mu_0)) \right] e^{-\delta 0/\mu 0} \quad \textbf{(7)}$$

is basically the same as Equation (6), with the exception of the direct transmission term.

Assuming that the shaded and unshaded regions are both a homogenous surface, the difference in radiance is,

$$L_s^{unshaded} - L_s^{shaded} = L_d = \frac{r_s}{1 - r_s \bar{r}} \frac{\mu_0 F_0}{\pi} e^{-\delta 0 \left(\frac{1}{\mu 0} + \frac{1}{\mu} \right)}. \quad \textbf{(8)}$$

So, solving Equation (8) for Total Optical Depth (TOD) yields,

$$\delta_0 = \left(\frac{\mu_0 \mu}{\mu + \mu_0} \right) \ln \left[\left(\frac{r_s}{1 - r_s \bar{r}} \right) \left(\frac{\mu_0 F_0}{\pi L_d} \right) \right]. \quad \textbf{(9)}$$

where δ_0 is total optical depth, μ_0 is the cosine of the solar zenith angle, μ is the cosine of the sensor zenith angle, r_s is the surface reflectance, $\bar{r}$ is the mean aerosol reflectance (MAR), F_0 is the spectral solar irradiance for the specific channel, and L_d is the difference between the nonshadow and shadow radiance. The equation for calculating TOD is derived from Liou's (2002) development of the principles-of-invariance (POI) method to describe the multi-scattering problem.

3. Molecular Rayleigh Scattering Optical Depth Calculation

In order to derive an accurate AOD measurement from the TOD, a correction is applied that accounts for the optical depth due to Molecular Rayleigh Scattering. Russell et al. (1993) provides a well documented approach to calculating Rayleigh Optical Depth (ROD) values dependent on wavelength, pressure and height:

$$\delta_R(\lambda) = \left(0.00864 + 6.5\times10^{-6}H\right)\lambda^{-b(\lambda)}\left(p/p_0\right) \quad \textbf{(10)}$$

$$b(\lambda) = 3.916 + 0.074\lambda + 0.050/\lambda \quad \textbf{(11)}$$

Where H is the height above sea level of the radiometer (km), p is the atmospheric pressure at the height of the radiometer (hPa), λ is the wavelength (micrometers) and p_o is the sea level reference pressure, one standard atmosphere (1013.24 hPa).

4. Calculating Aerosol Optical Depth (AOD)

Equation (9) provides a useful tool for measuring TOD. Most of the variables are either known and the radiance difference between the shadow and nonshadow region (L_d) and the surface reflectance (r_s) are measured from the image. Solar and sensor zenith angles can be found using the Terascan software suite. The solar irradiance (F_0) is constant for the specific channel being used, 1621 and 924 $Wm^2\mu$ for Band 1 and Band 2, respectively.

Deriving AOD is an iterative approach well outlined in Vincent's research. Basically, once the needed variables are collected, a first iteration of TOD is calculated under the assumption the mean surface reflectance (r_s) is much larger than the aerosol reflectance ($\bar{r}$). This allows the top-of-the-atmosphere (TOA) reflectance to be used as the surface reflectance in the shadow region.

Once the first iteration of TOD is obtained, it can be used in the following equation to find the Mean Aerosol Reflectance (MAR),

$$\bar{r} = \frac{1}{\pi}\int_0^{2\pi}\int_0^{1}\int_0^{2\pi}\int_0^{1}\frac{\tilde{\omega}\mu'\mu''}{\mu'+\mu''}\left(\frac{P(\Theta)}{4\pi}\right)\left(1-e^{-\delta\left(\frac{1}{\mu'}+\frac{1}{\mu''}\right)}\right)d\mu' d\phi' d\mu'' d\phi'' \qquad \textbf{(12)}$$

where $\tilde{\omega}$ is the single scatter albedo, δ is the TOD and $P(\Theta)$ is the scattering phase function.

The scattering phase function in this case is the Henyey-Greenstein phase function,

$$P(\Theta) = \frac{1-g^2}{\left(1+g^2-2g\cos\Theta\right)^{3/2}} \qquad \textbf{(13)}$$

where Θ is the scattering angle and *g* is the asymmetry parameter that can range from -1 to 1, fully backscattered condition to fully forward scattered, respectively. Values fro the single scatter albedo and the asymmetry parameter can be assumed based on expected aerosol type, although Vincent shows that the AOD values do not vary greatly with changes to $\tilde{\omega}$ or g. Total uncertainty for the Shadow Method is typically ±0.04 optical depth units based on the assumption in $\tilde{\omega}$ and g, but in extreme cases can be as high as 0.10 optical depth units. The MAR is determined using a numerical approach to the quadruple integral in Equation (12). MAR approximates the diffuse sky radiance.

Once the MAR is calculated, it can be subtracted from the top of the atmosphere reflectance to solve for the mean surface reflectance. Since r_s and $\bar{r}$ are known, a second and final iteration of TOD can be calculated. Once the final TOD is calculated, the ROD (Equation 10) is subtracted and we finally get a value for AOD.

C. MODIS

Previous research by Waghelstein used hyper-spectral imagery from TACSAT. There were several limitations. The first was that the data was classified. The second was that most of the satellite passes were over areas nowhere near NASA Aeronet sites. Three locations happened to be within 10km, but were urban areas. While urban areas provide good shadows, the problem is that the surfaces were not all homogeneous. Shadows cast

by buildings encompassed other buildings, roads, houses, etc. This research focused on desert areas that had shadows cast by clouds and terrain. The cases used definitely had homogeneous surfaces, but one drawback to using desert regions is that other than a dust storm, the aerosol content is low. Initial research was focused on finding HS imagery, but classified data could not be transferred to removable media and ordering images required Artemis to mail data discs. It was then where the focus switched to using MODIS imagery.

III. METHODOLOGY

A. OVERVIEW

The Shadow Method was developed with the intent of exploiting regions of shaded and unshaded radiance found in high resolution imagery. Vincent stated that the image would have to be orthorectified and calibrated for the Shadow Method to retrieve accurate AOD values. Follow-on research by Rivenbark (2009) would later prove that the time-consuming orthorectification process played no part in the constant low-bias and could therefore be ignored in pre-processing stages. Shadow and non-shadow pairs were manually collected by the user in the Environment for Visualizing Images (ENVI) version 4.7 software suite and run through a customized code in Mathwork's Matrix Laboratory (MATLAB) software that calibrated the image and calculated AOD values.

B. SATELLITE IMAGERY

1. Imagery Retrieval

Each case in this research was obtained from the United States Geological Survey (USGS) through the NASA Land Process Distributed Active Archive Center (LP DAAC). The files can be ordered through their website at https://lpdaac.usgs.gov.

2. ROI Sampling

Using the ENVI software suite, Regions of Interest (ROI) were sampled. The user would load the appropriate image file and identify regions of shadow/non-shadow pairs. It is very important that the user choose to analyze the image in radiance, not reflectance. The ROI statistics function allows the user to isolate regions in the scene. Once the region is selected, the user then views the "stats" function. There, the user can see the maximum, minimum, mean and standard deviation values of brightness values for each pixel for the particular region. The user must save the data as a text file in order for MATLAB to read it. As proven by Dombrock (2007) and Evans (2008), AOD values were most accurate

when compared to the mean calibrated radiance value within each ROI pixel, as opposed to a minimum, maximum or mode sampling values.

In order to pick the shadow/non-shadow pairs that would yield the best results, care must be taken by the user. Dombrock (2007) and Rivenbark (2009) showed that shadow ROIs selected within the center of the shadow produced better results than selecting large portions of the shadow or near the edge of the region.

3. AOD Calculation

The MATLAB code was originally written in the Interactive Data Language (IDL) for ENVI by Vincent (2006) and later altered by Dombrock (2007) and Rivenbark (2009). In 2010, Waghelstein translated the code into MATLAB language due to the spectrally robust ARTEMIS Hyper-Spectral sensor and the software's matrix math capability. Since MODIS has only two bands compared to ARTEMIS's 480 bands, the code was manipulated once again. Waghelstein's entire code took roughly 50 minutes to compile results. Using the MODIS sensor's two bands, the code only takes about three seconds.

In order to "simplify" the code, multiple changes were made. Due to the 480 bands that Wagelstein used, each wavelength for each respective band was pulled from the Whereli excel file. Using MODIS, the central effective wavelength could just be set at 0.650 and 0.860 for Band 1 and Band 2, respectively. The scale factor, a variable for the aperture radiance calibration, was made a constant because the images were already in terms of radiance.

It is recommended that the user identify as many pairs as possible. With multiple ROIs selected for each image file, the user is able to save the statistics output into an ASCII text file. Using the "total_shadowtype.m" MATLAB file, the ASCII text files are imported into the code that would calculate AOD values for each shadow/non-shadow pair.

Since editing the code can get cumbersome, it is recommended the user make separate .m files to isolate the type of shadow that is being derived, for example, cloud

and terrain. Before the code can be run, the user is required to find the solar and zenith angles using the Terascan software suite, the number of pairs being investigated, the Julian day and ground truth for both bands. Once the code is run, results are displayed in nearly three seconds in terms of the AOD for each shadow/non-shadow pair, separated by wavelength band.

THIS PAGE INTENTIONALLY LEFT BLANK

IV. RESULTS

A. FT. HUACHUCA, DECEMBER 23, 2009

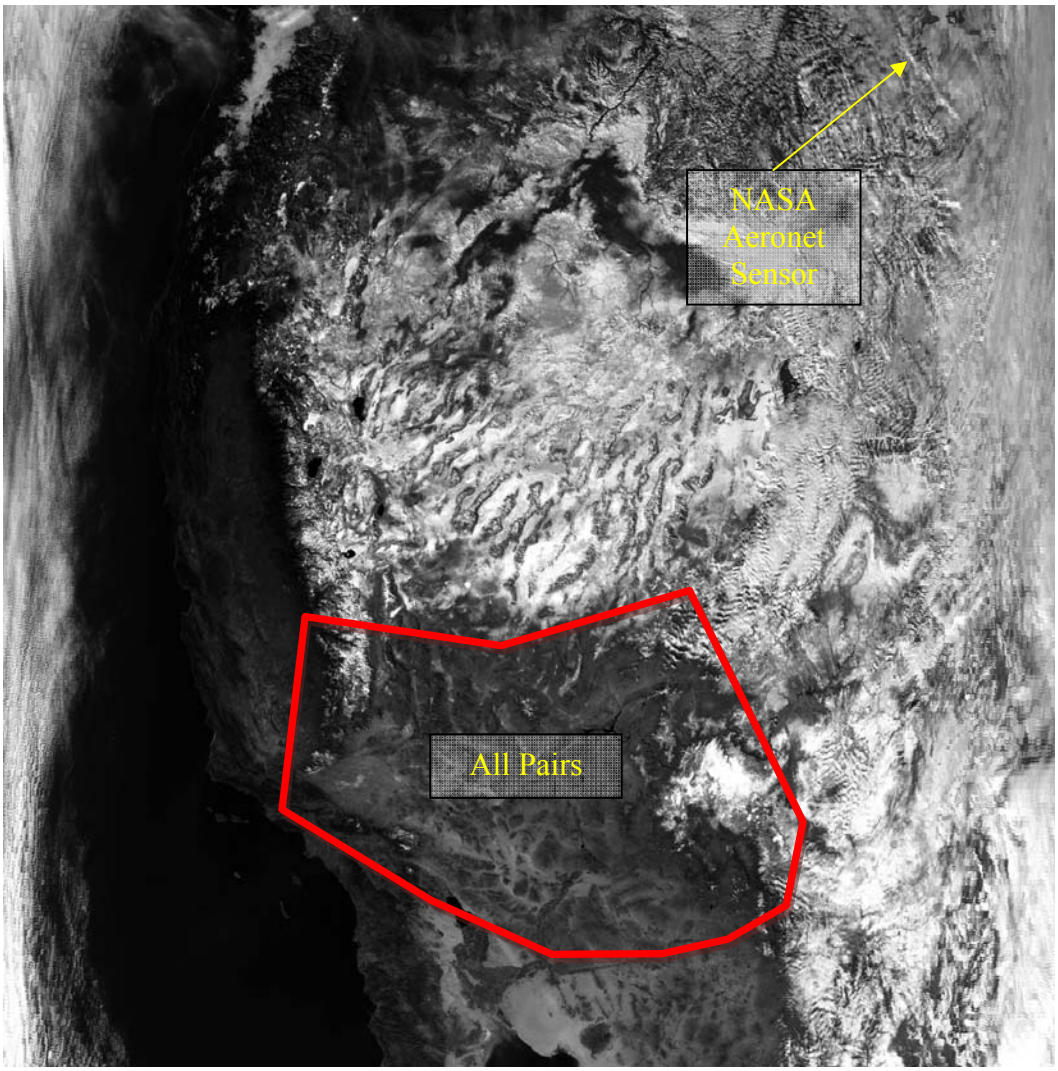

Figure 2. MODIS Image of Fort Huachuca, December 23, 2009. All terrain and cloud pairs were taken from the annotated area.

1. Overview

The first case analyzed was at Fort Huachuca on December 23, 2009. This site was originally chosen using the Hyperspectral imagery from the ARTEMIS sensor because of its close proximity to a NASA AERONET sensor. The image was ordered, but could not be mailed due to classified restrictions. The same image could have been ordered from the MODIS site. This scene was ideal because it had both cloud and topography shadows. All of the pairs were taken from the northern section of the image, along the cloud border (Figure 2).

2. Hypothesis

The original hypothesis was that all Shadow Method-derived AOD values, both cloud and terrain-generated, would be within 0.05 units of the NASA AERONET ground truth data. I also expected the range of values to be small, within 0.02 units. Since the entire scene is fairly homogenous, cloud and terrain-generated shadows were used that had shadows larger than 30 pixels. Shadows any smaller than 30 pixels would be difficult to analyze using the ROI tool.

3. Cloud

In all result figures, each symbol represents the Average AOD for a particular shadow/non-shadow pair. The values for the cloud pairs range from close to zero to 0.06 for Band 1 and 0.03 to 0.09 for Band 2 (Figure 4). Band 2 is higher in all cases due to the mathematics. The Central Effective Wavelength (CEW) for Band 1 and Band 2 is 0.650 and 0.860 respectively. This makes the Rayleigh Optical Depth (ROD) larger for Band 2. The solar irradiance (F_0) is 1621 and 924 $Wm^2\mu$ for Band 1 and Band 2, respectively. (F_0) is in the denominator of the "albedo1" function in the code, making Band 2 larger.

The ground truth from the AERONET sensor was 0.095 and 0.10 for Band 1 and Band 2, respectively. These are very low values for AOD. This was expected due to the location of Fort Huachuca, which is far from any urban area and apart from clouds, was clear with respect to smoke, dust and pollution.

Pairs 2, 4 and 6 yielded the results closest to the ground truth. This is due to greater contrast in radiance between the shadow and non-shadow area. These pairs were within the 0.05 AOD unit expectation. Pair 1 appeared to have white sand in the scene (Figure 3A). This area of higher albedo has a higher reflectance, lessening the contrast between the shadow and non-shadow region. Pair 3 incorporated a very small shadow of 24 pixels (Figure 3B) and pair 5 was surrounded by cloud (Figure 3C). Higher resolution imagery could have produced more accurate results.

Pair 7 is consistent with what Dombrock (2007) and Rivenbark (2009) showed in their research where ROIs selected within the center of the shadow provided better results than selecting large portions of shadow near the base of the generator or the edge of the shadow/non-shadow region. The shadow region selected in this scene was very close to the border (Figure 3E). The differences are rather small, but considering the AOD was around 0.10, values above zero using the shadow method are encouraging. The level of uncertainty with the range of values was perplexing, even though it is consistent with what Vincent showed with total uncertainty for the Shadow Method is typically ±0.04 optical depth units. Ideally, the AOD values should have been analogous. The regions that were sampled were taken in close proximity to one another and the user assumed that the atmosphere was homogenous. It was concluded that the variation in the results were caused by the shadow generator or the characteristics of the surface. The scenes that were selected appeared to be mostly homogenous, with only minor differences in the terrain. This led to the analysis of regions with terrain-induced shadows.

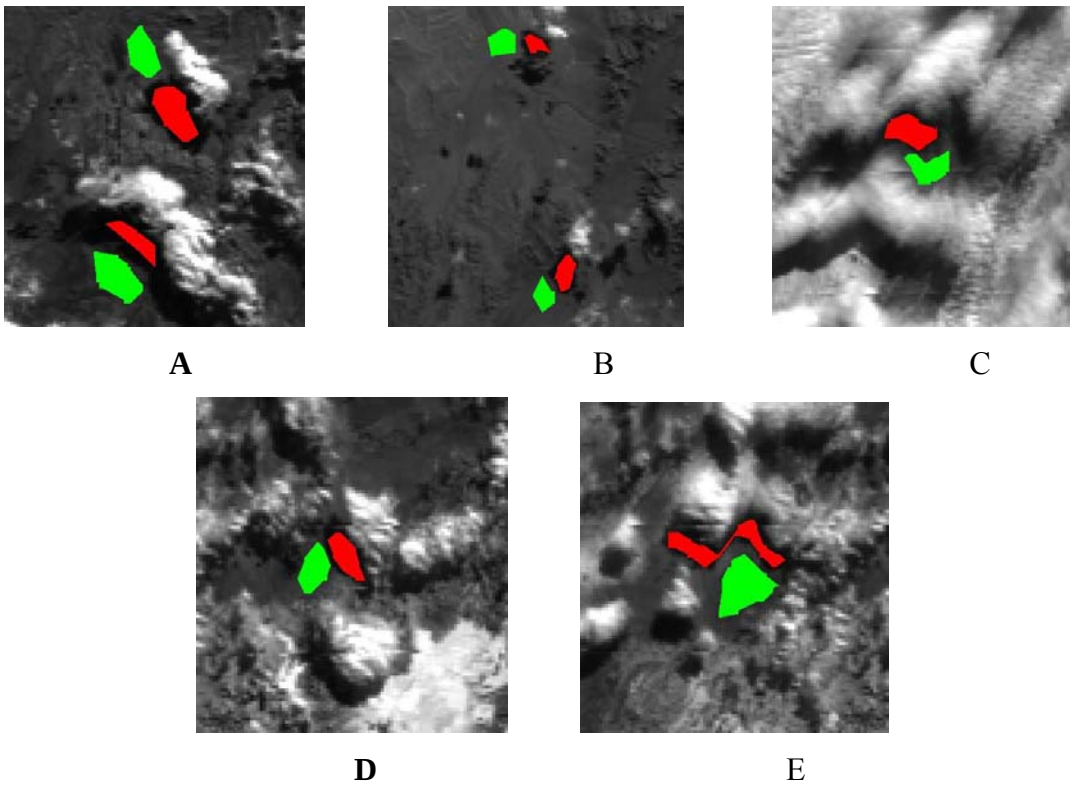

A B C

D E

Figure 3. Cloud pairs from Fort Huachuca, December 23, 2009. A) Pair 1 (top) and Pair 2. B) Pair 3 (top) and Pair 4. C) Pair 5. D): Pair 6. E) Pair 7.

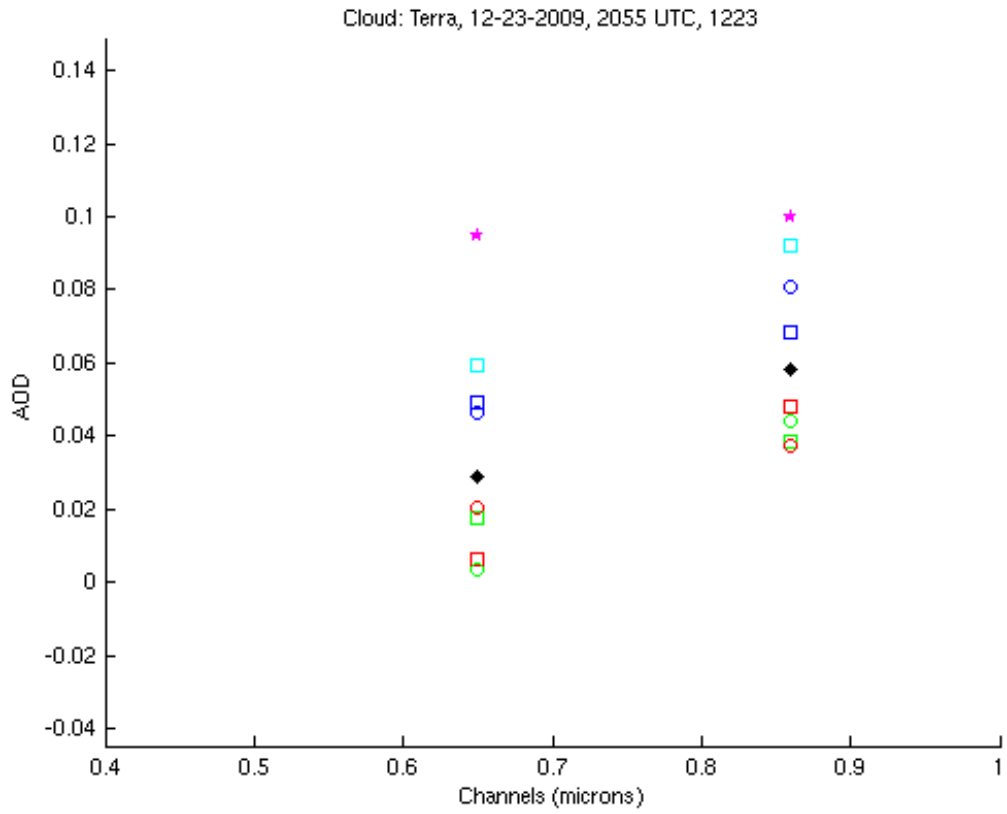

Figure 4. MATLAB results from Fort Huachuca Cloud Pairs, December 23, 2009. Pair 1: red square, Pair 2: blue square, Pair 3: green square, Pair 4: aquamarine square, Pair 5: red circle, Pair 6: blue circle, Pair 7: green circle, Pair 8: aquamarine circle, Computed Average AOD: black diamond, NASA AERONET AOD (Ground Truth): Pink Star.

4. Terrain

The AOD values from the terrain cases were not as close to the ground truth as the cloud results (Figure 6). Only the fourth pair was within the 0.05 AOD unit expectation. However the range of values is much smaller. This is due to characteristics of the shadow generators. The terrain is homogenous, compared to the cloud generators. With cloud, radiation can get through, allowing some to reach the ground where it could be reflected up to the sensor. With terrain, radiation cannot get through the shadow generator, making the shadow a "true" shadow. The low AOD values, compared to the cloud results could be due to the size of the shadow pairs. The average number of pixels for each pair was about 32, compared to the cloud scenes of 100. This limited the user

from avoiding the edge of the shadow. Dombrock (2007) and Rivenbark (2009) showed that shadow ROIs selected within the center of the shadow produced better results than selecting large portions of the shadow or near the edge of the region. The results were much more grouped and Band 1 was lower, as expected. The values for the results in Band 2 were higher, but still less than half of what the AERONET sensor recorded. Pair 4 yielded the lower results due to the snow near the shadow region (Figure 5C). Just like with the cloud case with pairs 1, 3 and 5, higher albedo in the shadow region seem to reduce the contrast between the shadow and non-shadow regions. The area of snow was analyzed as the non-shadow, but the area was only 20 pixels. The range of values in this case was more impressive due to the tight grouping, but not convincing for accurate Shadow Method-derived AOD values. The ground truth value of 0.10 essentially shows that the air was clear and no significant value of AOD could be obtained.

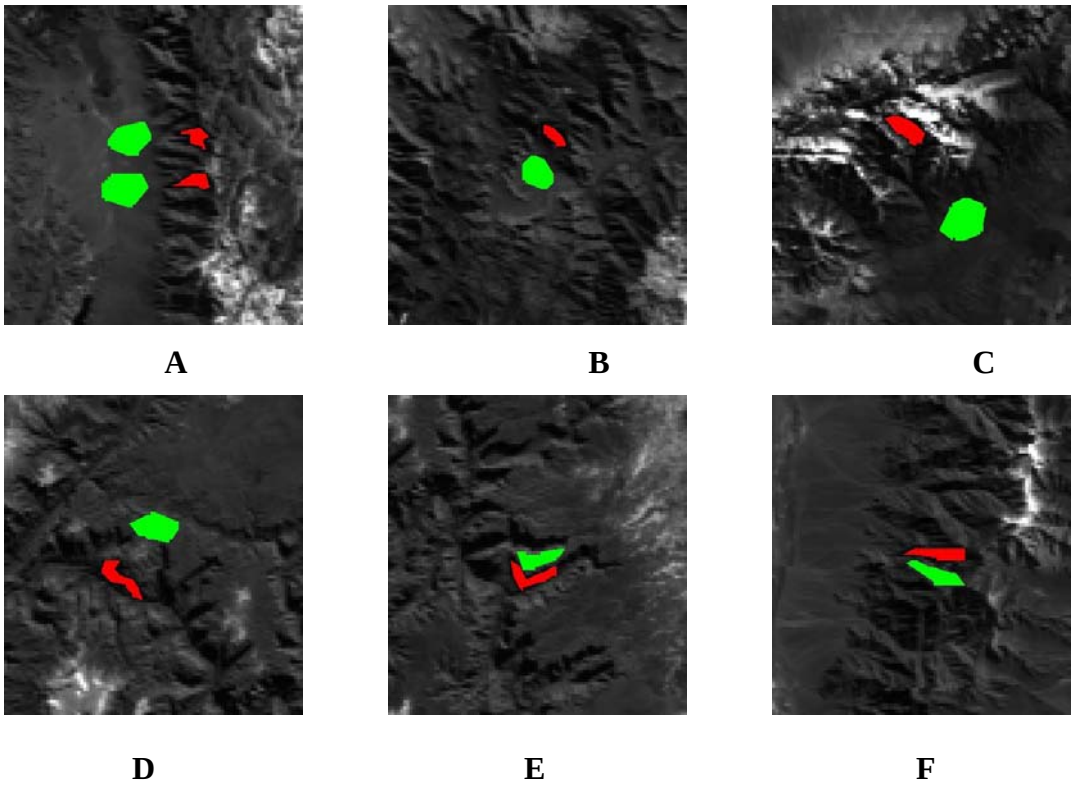

Figure 5. Terrain Pairs from Fort Huachuca, December 23, 2009. A) Pair 1 (top) and Pair 3. B) Pair 2. C) Pair 4. D): Pair 5. E) Pair 6. F) Pair 7.

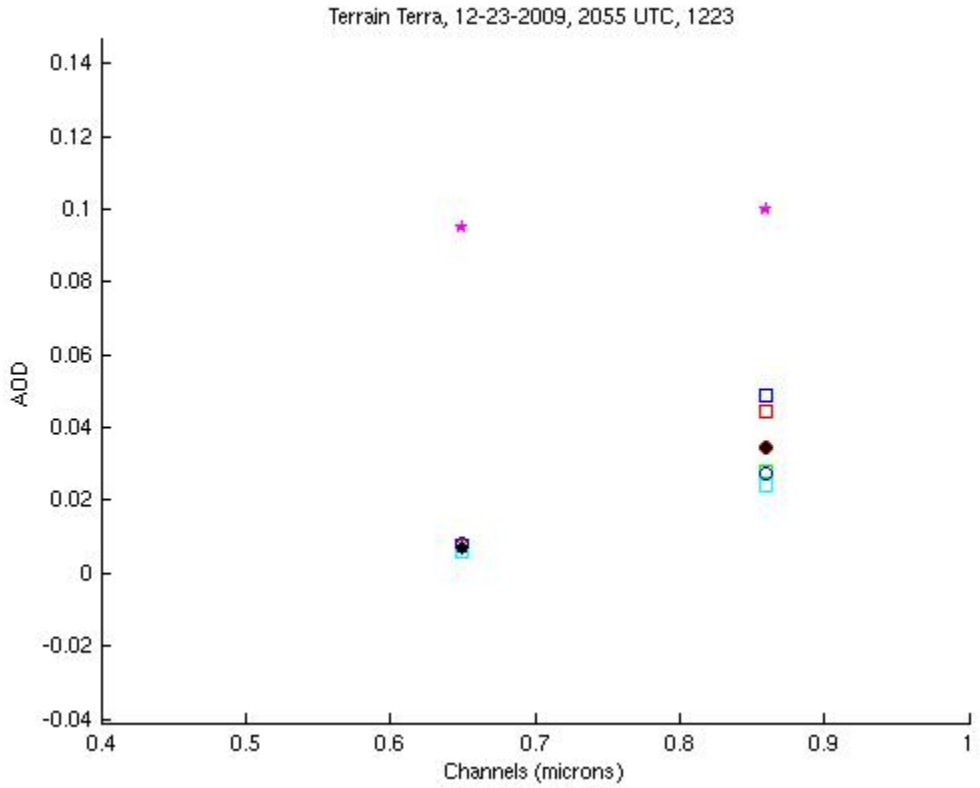

Figure 6. MATLAB results from Fort Huachuca Terrain Pairs, December 23, 2009. Pair 1: red square, Pair 2: blue square, Pair 3: green square, Pair 4: aquamarine square, Pair 5: red circle, Pair 6: blue circle, Pair 7: green circle, Computed Average AOD: black diamond, NASA AERONET AOD (Ground Truth): Pink Star.

B. SAUDI ARABIA, DECEMBER 12, 2003

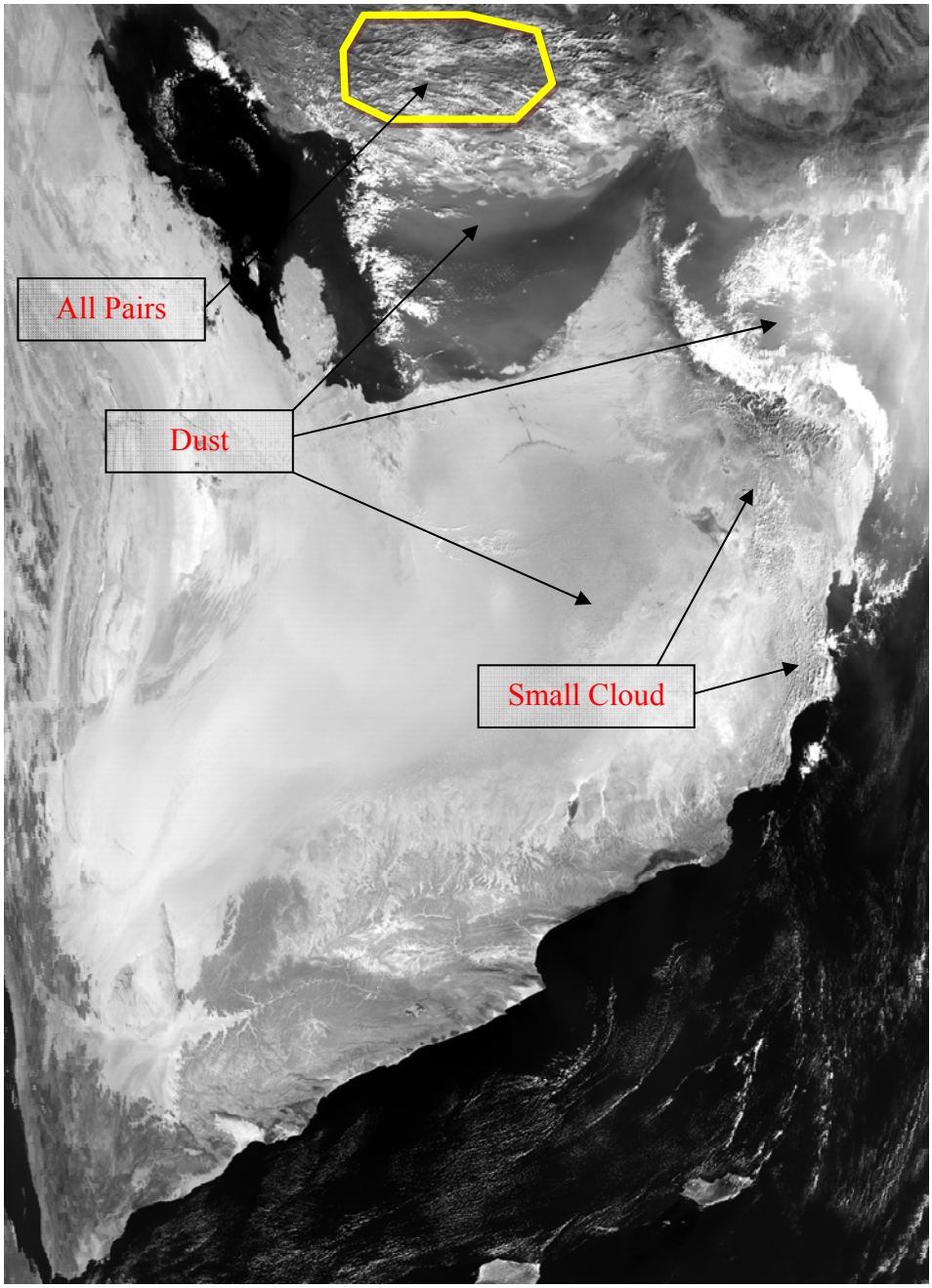

Figure 7. MODIS Image of Saudi Arabia, December 12, 2003, 0710 UTC. All cloud pairs were taken from the yellow-annotated area.

1. Overview

After seeing the results from the Fort Huachuca case, it was decided to analyze cases that were known to have higher AOD values. A dust storm over Saudi Arabia on December 12, 2003 was chosen (Figure 7). The image was taken at 0710 UTC, which is 1140 local time. Shadows are hard to come by at this time because the sun is almost directly overhead at noon. Shadows were found, but mostly in the northern portion of the image. Shadows generated by terrain could not be found because the region is mostly flat.

2. Hypothesis

Since ground truth could not be obtained, A different approach had to be taken. Since this is a region of high AOD, it was desired to retrieve Shadow Method-derived values larger than the previous case. Even though the area that was sampled was in a clearing area, the values should be larger than 0.10. The previous case showed that results vary on the characteristic and size of the shadow generator. The goal of this case was to show that the Shadow Method could produce results larger than 0.10. With respect to the range of values, 0.05 was acceptable like the previous case since not all clouds are the same.

3. Cloud

Clouds were present on the southeastern edge of the image, but were too small to try, roughly 10 pixels. Noon is early in the day and the clouds were just beginning to form. After looking over the entire image, shadows large enough for using the ROI tool were found over Southwestern Iran. Four pairs were analyzed that yielded an AOD average of 0.065 (Figure 9). These values seem low and make sense due to the clearing area in the north. Similarly to the first case, the results were higher for Band 2.

Pair 1 has a lower value due to the thickness of the cloud (Figure 8A). The cloud appears to have a lower brightness temperature. This means that the cloud is warmer in temperature and not as thick, allowing more radiation to reach the ground. The cloud is thick enough to cast a shadow, but the radiance difference is not as great as the other

three pairs. Pairs 2, 3 and 4 clearly show brighter clouds, indicating higher cloud tops. Since these pairs were taken fairly close to each other, it is assumed that the Lifted Condensation Level, the level where clouds form, is the same. If the cloud base level is the same, then brighter cloud tops would indicate thicker clouds.

The take-away from this case is encouraging because the Shadow Method does yield results, but just like the Fort Huachuca cloud case, they do vary based on the characteristics of the shadow generator. With the exception of the first pair, I was pleased with the values and range of values. Pairs 2, 3 and 4 were within 0.02 of each other, exceeding my expectations. If the image was taken later in the day, perhaps terrain-generated shadow scenes could have been analyzed. The more shadow pairs the user can find, the more accurate the AOD average will be. Since four pairs were analyzed here, the range of results was quite large. Ground Truth could not be obtained due to the fact that most countries, like Iran, are not forthcoming with their weather data or cannot afford the technology to share their data.

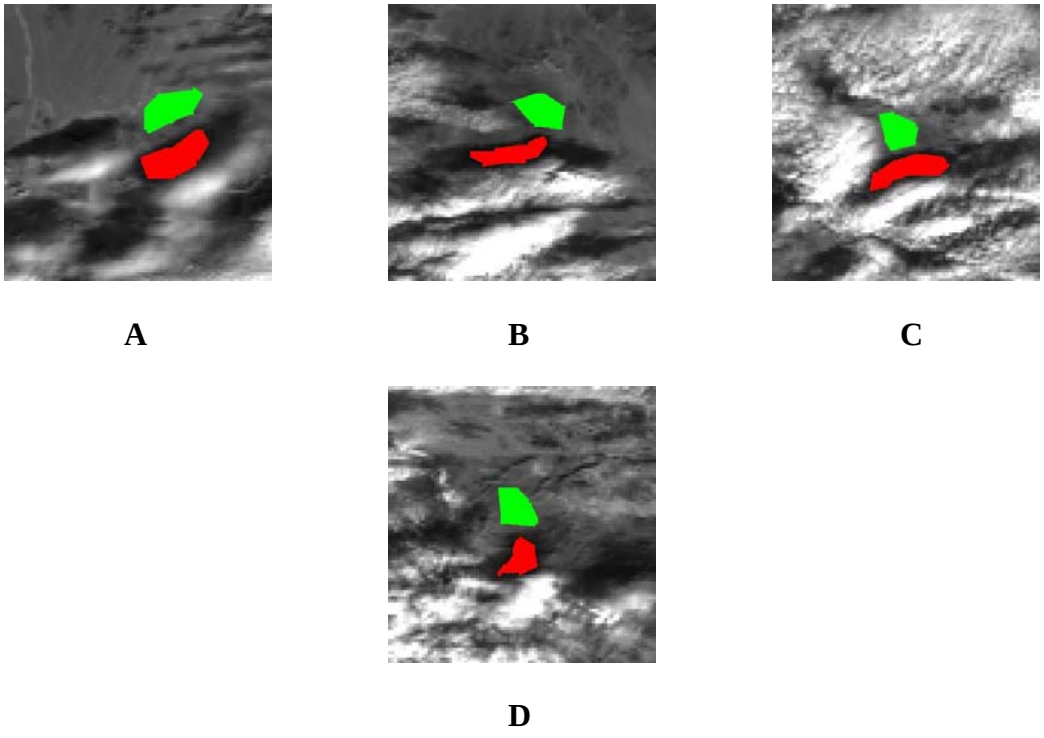

Figure 8. Cloud Pairs from Southern Iran, December 12, 2003. A) Pair 1. B) Pair 2. C) Pair 3. D): Pair 4.

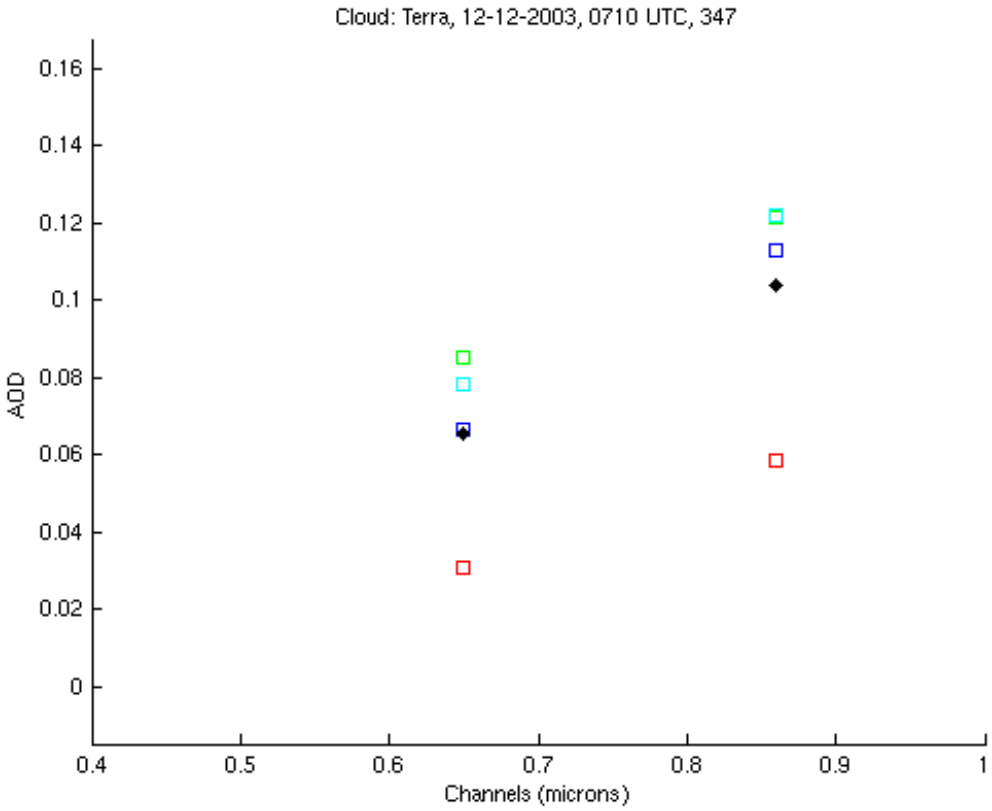

Figure 9. MATLAB results from Saudi Arabia Cloud Pairs, December 12, 2003. Pair 1: red square, Pair 2: blue square, Pair 3: green square, Pair 4: aquamarine square, Computed Average AOD: black diamond.

C. IRAN/AFGHANISTAN, DECEMBER 11, 2003

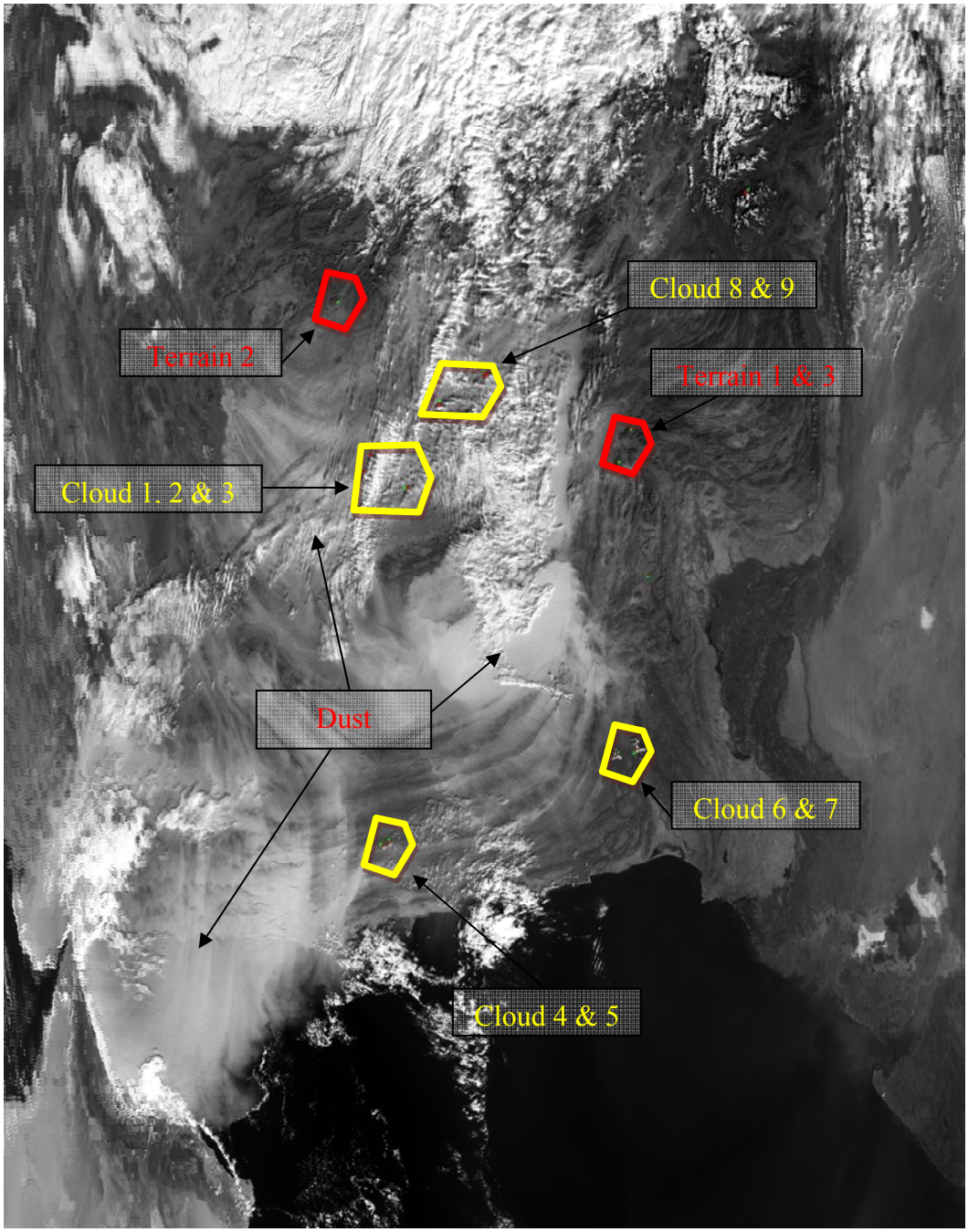

Figure 10. MODIS Image of Iran and Afghanistan, December 11, 2003, 0625 UTC. All cloud pairs were taken from the yellow-annotated areas. Terrain pairs were taken from the red-annotated areas.

1. Overview

The third and final case analyzed was the same region as the second case, but 23 hours later. The satellite pass at this time was also further northeast. This image is ideal because it had more shadow generators, both due to cloud and terrain. These areas also varied in that they lay in areas of high and low AOD due to the dust storm (Figure 10). Shadows could not be analyzed in the thicker areas of dust. As with the previous case, ground truth could not be obtained.

2. Hypothesis

Since this scene has varying regions of AOD, the goal was to show that areas in the vicinity of the dust storm could produce distinctively higher Shadow Method-derived AOD values for both the cloud and terrain-generated pairs. Using 0.10 as a minimum value made sense, since it was used in the previous two cases. The range of values, however, needs to be looked at differently, since the scene varies. A large range of values for both the cloud and terrain-generated shadow pairs was acceptable because a large portion of the scene was sampled.

3. Cloud

This case produced higher results, compared to the previous case. Values ranged from 0.07 to 0.29, the highest results of all three cases (Figure 12). Pairs 1–3 and 6–9 yielded the lowest results. Taking a closer look at Figures 11E–F, it is obvious that pairs 6 and 7 are clearer than the others. This is also evident in Figure 10. There is some dust over the scene, but not much. These values are somewhat close to the values for pairs 1–3 and 8–9, even though there is less dust. The reason for this is similar to the previous case in that cloud characteristics play a role. In Figures 11E–F, the brightness temperature is higher than the others. This indicates thicker clouds, which means that the cloud is allowing less radiation to reach the surface. So, the shadow is darker for pairs 6 and 7, making the difference between the shadow/non-shadow regions greater, giving a higher value for AOD. If the clouds were all the same, then pairs 1–3 and 8–9 would show greater AOD values, since there is more dust over those scenes.

Pairs 4 and 5 yielded the highest results (Figure 12) because this region was surrounded by the dust storm (Figure 10). The brightness temperature for this scene is lower, but the dust content is greater, which won out. If the clouds were as thick as pairs 6 and 7, the AOD values would have been even greater.

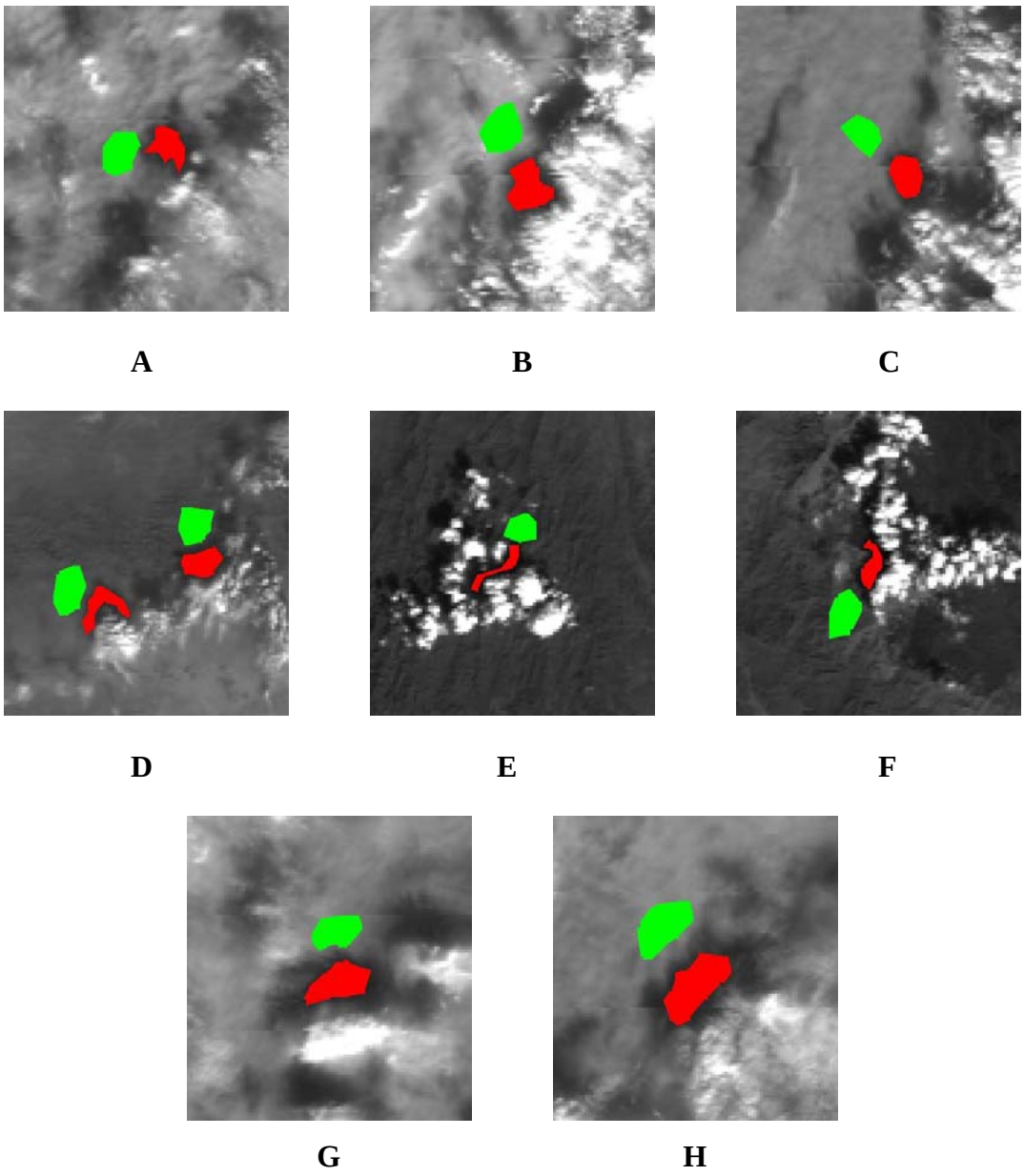

Figure 11. Cloud Pairs from Iran and Afghanistan, December 11, 2003. A) Pair 1. B) Pair 2. C) Pair 3. D): Pair 4 (left) and Pair 5. E) Pair 6. F) Pair 7. G) Pair 8. H) Pair 9.

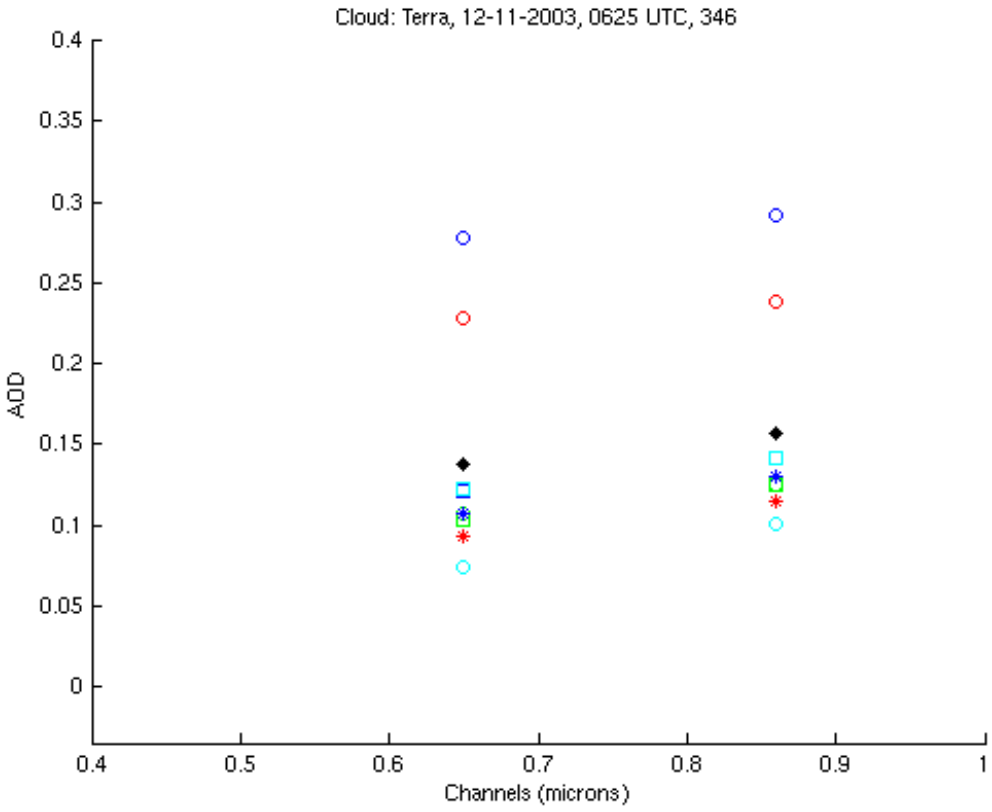

Figure 12. MATLAB results from Iran/Afghanistan Cloud Pairs, December 21, 2003. Pair 1: blue square, Pair 2: green square, Pair 3: aquamarine square, Pair 4: red circle, Pair 5: blue circle, Pair 6: green circle, Pair 7: aquamarine circle, Pair 8: red star, Pair 9: blue star, Computed Average AOD: black diamond.

1. Terrain

Three pairs of terrain scenes were analyzed in Afghanistan. These areas were not in the thick portions of the dust storm (Figure 10). The images appear as clear as the cloud pairs in Figure 11E–F. The values for those cloud pairs (6 &7) in Band 2 ranged from 0.10 to 0.125 (Figure 13) and the values for this terrain case ranged from 0.05 to 0.125 in Band 2 (Figure 14). Even though the cloud and terrain pairs were analyzed in different areas, they should exhibit similar AOD values.

Pair 2 exhibited the higher results due to the scene being on the northern edge of the dust storm (Figure 10). The area was clearing, but aerosols were still present. Pairs 1

and 3 are on the eastern edge of the storm and judging by the northwesterly wind direction, have not been greatly affected yet. If the image were taken an hour later, AOD results would have been higher.

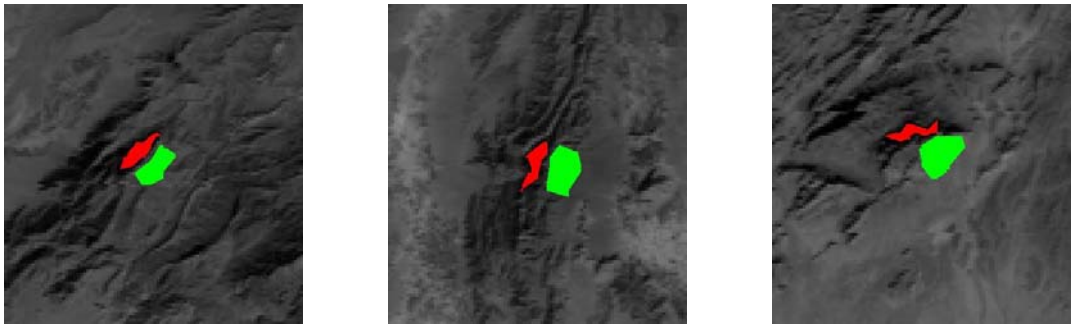

A **B** **C**

Figure 13. Terrain Pairs from Afghanistan, December 11, 2003. A) Pair 1. B) Pair 2. C) Pair 3.

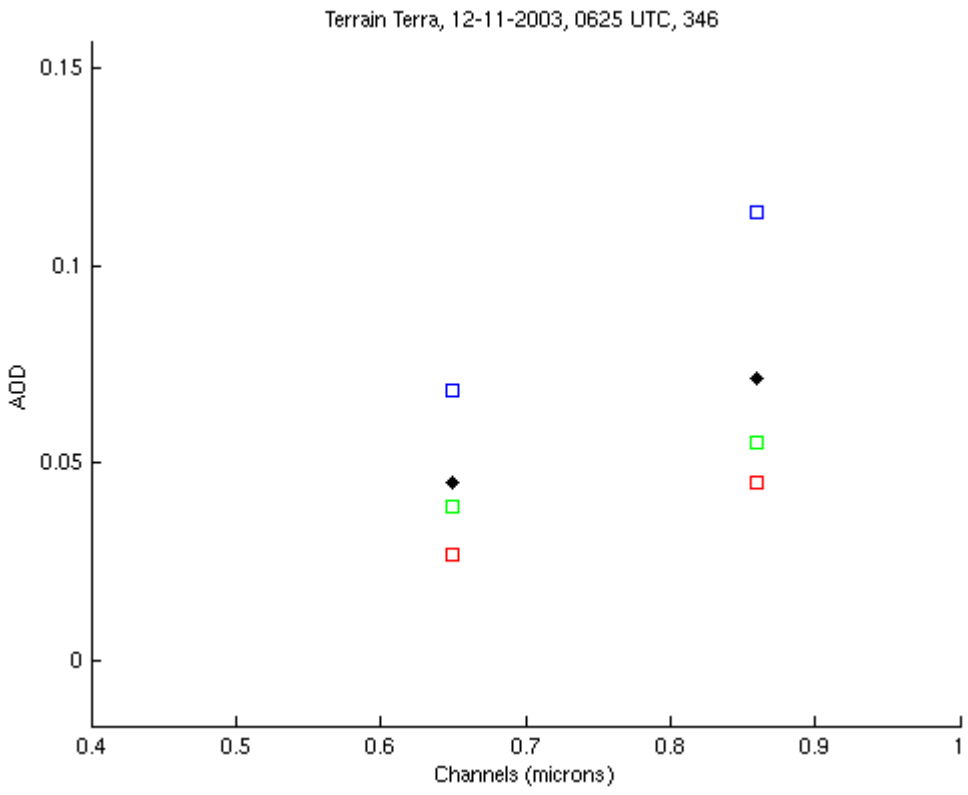

Figure 14. MATLAB results from Afghanistan Terrain Pairs, December 21, 2003. Pair 1: red square, Pair 2: blue square, Pair 3: green square, Computed Average AOD: black diamond.

THIS PAGE INTENTIONALLY LEFT BLANK

V. CONCLUSION

A. FINDINGS

All three cases provided varied results. Fort Huachuca was analyzed on a very clear day. The results were low, but greater than zero, which was encouraging. The cloud-generated shadow pairs theoretically should have been similar to one another, but were varied depending on the characteristic of the cloud. One would not believe any worth can come from cloud-generated shadow analysis. Values can be retrieved, but how reliable would they be? Not all clouds in a scene are the same, so one would get varied AOD values in an area that should get the same. The Afghanistan case is a good example of this. In an area of thick dust, the Shadow Method-derived AOD for cloud pairs 8 and 9 should have much higher, but was low due to the cloud thickness. One would need to know the cloud depth and be certain that the shadow is genuine.

For the Fort Huachuca case, the terrain pairs could have been higher if the shadow regions were larger, but all seven pairs had nearly identical AOD values making the uncertainty low, but accuracy was also poor. Perhaps if the AOD was higher, more convincing results could have been found.

Both the Saudi Arabia and the Afghanistan cases proved that the shadow method does, in fact produce results. Apart from different cloud characteristics, both cases yielded results that made sense. Areas of intense dust had higher AOD results than the areas that were clear. The terrain case for Afghanistan produced similar AOD values and it is supported that both this case and the Fort Huachuca terrain case produced more trustworthy results.

B. UNCERTAINTY

While the cloud cases provided the higher results for all three scenes, the results were varied based on cloud characteristics. Scenes that should have yielded higher AOD values like the Iran and Afghanistan cases ended up producing lower results due to decreased cloud thickness. If one were to try to retrieve AOD using the shadow method, care must be taken by the user. Areas of high AOD could be underestimated if the clouds are not thick enough.

C. RECOMMENDATIONS AND FOLLOW-ON RESEARCH

For the next round of research, two avenues are recommended. Since this research showed that the terrain-generated shadow scenes produced more consistent results, the first recommendation would be to find cases that have high AOD scenes with many terrain-generated shadows. Ideally, these scenes should be close to a ground truth source. The time of day should also be taken into consideration. Images taken around noon would provide smaller shadow regions, so early morning or mid-afternoon would be ideal.

The second round of research would be to look into what cloud depth would provide the more accurate AOD. The three cases in this research had more cloud pairs than terrain pairs, so a greater number of cases could be analyzed. In order to do this, one would need ground truth and upper air data to confirm atmospheric conditions.

LIST OF REFERENCES

Belson, B. L., 2010: A Fully Automated Method of Locating Building Shadows for Aerosol Optical Depth Calculations in High Resolution Satellite Imagery. PhD thesis. Dept. of Meteorology, Naval Postgraduate School, Monterey, CA.

Dombrock, R. M., 2007: Automating the Shadow Method For Aerosol Optical Depth Retrieval. M.S. thesis, Dept. of Meteorology, Naval Postgraduate School, Monterey, CA.

Evans, J. R., 2007: A Verification of Optical Depth Retrievals From High Resolution Satellite Imagery. M.S. thesis, Dept. of Meteorology, Naval Postgraduate School, Monterey, CA.

Hermosillo, AZ, cited Dec 2009: Aerosol Robotic Network (AERONET) mission. <Available online at http://aeronet.gsfc.nasa.gov>

Hsu, N. C., S. C. Tsay, M. D. King, and J. R. Herman, 2004: Aerosol Properties Over Bright-Reflecting Source Regions. *IEEE Trans. Geosci. Remote Sens.*, 42, 557–569

Kaufman, Y. J. and J. H. Joseph, 1982: Determination of Surface Albedos and Aerosol Extinction Characteristics From Satellite Imagery. *J. Geophys. Res.*, 87, 1287–1299.

Liou, K. N., 2002: *An Introduction to Atmospheric Radiation*. Academic Press, pp. 583.

MODIS Specifications. NASA. <Available online at http://modis.gsfc.nasa.gov>

Odell, A. P. and J. A. Weinman, 1975: The Effect of Atmospheric Haze on Images of the Earth's Surface. *J. Geophys. Res.*, **80**, 5035–5040.

Rivenbark, B. J., 2009: Investigation of Panchromatic Satellite Imagery Sensor Low Bias in Shadow Method Aerosol Optical Depth Retrieval. M.S. thesis, Dept. of Meteorology, Naval Postgraduate School, Monterey, CA.

Robles Gonzalez C., J. P. Veefkind, G. de Leeuw, 2000: Aerosol Optical Depth over Europe in August 1997 Derived From ATSR-2 Data. *Geophys. Res. Let.*, **27**, 955–958.

Seinfeld, John H., and S. N. Pandis, 2006. *Atmospheric Chemistry and Physics: From Air Pollution to Climate Change*. John Wiley & Sons

Sweat, P. C., 2008: Verification of Aerosol Optical Depth Retrievals From Cloud Shadows Using Satellite Imagery. M.S. thesis, Dept. of Meteorology, Naval Postgraduate School, Monterey, CA.

Vincent, D. A., 2006: Aerosol Optical Depth Retrievals From High-Resolution Commercial Satellite Imagery Over Areas of High Surface Reflectance. Dissertation, Naval Postgraduate School, Monterey, CA.

Veefkind, J. P., G. de Leeuw, P. Stammes, and R. B. A. Koelemeijer, 1998: Regional Distribution of Aerosol Over Land Derived from ATSR-2 and GOME. *Rem. Sens. Env*., 74, 377–386

Wehrli, C. 1985: *Extraterrestrial Solar Spectrum – Publ. 615.* Physical Meteorological Observatory and World Radiation Center, Davos Dorf, Switzerland.

Whagelstein, G. 2010: A Verification of Aerosol Optical Depth Retrieval Using the TACSAT-3 Satellite. M.S. thesis, Dept. of Meteorology, Naval Postgraduate School, Monterey, CA.

INITIAL DISTRIBUTION LIST

1. Defense Technical Information Center
   Ft. Belvoir, Virginia

2. Dudley Knox Library
   Naval Postgraduate School
   Monterey, California